These results imply that Lemma 3 provides a lower bound to $R_{LM}(D|q)$ and Lemma 4 an upper bound. Eliminating the common terms in eqns. 7 and 8 yields the lower limit T_l and upper limit T_u, respectively. Conversion is achieved if the difference between these two limits is less than a specified error ε. Blahut[8] presented an elegant proof (Theorem 6.3.8) guaranteeing conversion of the algorithm.

$R_{LM}(D|Q)$ algorithm:

(1) Specify the number of input intervals L, interval size α, output alphabet size M and output probabilities q_k and choose an arbitrary iteration vector Θ.

(2) Specify a slope s as input parameter and pre-calculate p_j, ρ_{jk} and $A_{jk} = e^{s\rho_{jk}}$.

(3) $\lambda_j = [\sum_k \theta_k q_k A_{jk}]^{-1}$; $c_k = \theta_k \sum_j p_j \lambda_j A_{jk}$; $\theta_k = [\sum_j p_j (A_{jk}/\sum_m \theta_m q_m A_{jm})]^{-1}$.

(4) $T_u = \sum_k q_k c_k \log c_k$ and $T_l = \max_k \log c_k$.

(5) If $|T_u - T_l| > \varepsilon$ return to step 3; else continue.

(6) $Q_{k|j} = \lambda_j \theta_k q_k A_{jk}$.

(7) $D = \sum_j \sum_k p_j Q_{k|j} \rho_{jk}$ and $R_{LM}(D|Q) = sD + \sum_j \log \lambda_j + \sum_k q_k \log \theta_k - q_k \log c_k$.

(8) Stop.

Results: Making use of the squared-error distortion measure, the algorithm has been applied to calculate $R_{LM}(D|q)$ for the unit-variance Gaussian probability, i.e. $q_k = 1/M$; $k = 1, 2, \ldots, M$. The results are shown in Fig. 1.

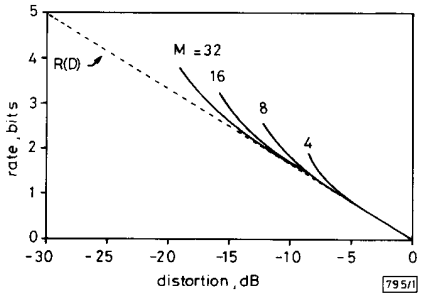

Fig. 1 *Alphabet-constrained rate-distortion function $R_{LM}(D|q)$ for unit-variance Gaussian probability density function for $M = 4, 8, 16$ and 32*

Discussion: For comparison the (unconstrained) rate-distortion function $R(D)$ is also shown in dotted lines, and since the distortion D is expressed in dB, $R(D)$ is a straight line. It is worth noting that the alphabet-constrained rate-distortion curves shown in Fig. 1 are an exact dual of Ungerboeck's[2] channel capacity curves for transmitting data through a bandwidth-limited channel. For each alphabet of size M there exists a unique minimum distortion, achievable only asymptotically at high rates, as previously shown by Finamore.[3] Considering the relatively small sizes of M and L, $R_{LM}(D|q)$ approaches $R(D)$ quite closely at low rates. In particular, at rates $R \leq 1$ bit/sample, which are most interesting for source encoding, the correspondence is remarkably good, thus guaranteeing TCQ performance close to the optimum promised by the rate-distortion function $R(D)$.

W. T. PENZHORN

Division of Microelectronics & Communications Technology, CSIR
PO Box 395
Pretoria 0001, South Africa

G. J. KÜHN

Department of Electronic & Computer Engineering
University of Pretoria
Pretoria 0002, South Africa

5th April 1989

References

1 MARCELLIN, M. V., FISHER, T. R., and GIBSON, J. D.: 'Predictive trellis coded quantization of speech'. Proc. IEEE int. conf. on Acoustics, Speech & Signal Processing, New York, April 1988, pp. 247–250

2 UNGERBOECK, G.: 'Channel coding with multilevel/phase signals', *IEEE Trans. Inf. Theory*, 1982, **IT-28**, pp. 55–67

3 FINAMORE, W. A., and PEARLMAN, W. A.: 'Optimal encoding of discrete-time continuous-amplitude memoryless sources with finite output alphabets', *IEEE Trans. Inf. Theory*, 1980, **IT-26**, pp. 144–155

4 PEARLMAN, W. A., and CHEKIMA, A.: 'Source coding bounds using quantizer reproduction levels', *IEEE Trans. Inf. Theory*, 1984, **IT-30**, pp. 559–567

5 FORNEY, JR., G. D.: 'The Viterbi algorithm', *Proc. IEEE*, 1973, **61**, pp. 268–278

6 BLAHUT, R. E.: 'Computation of channel capacity and rate-distortion functions', *IEEE Trans. Inf. Theory*, 1972, **IT-18**, pp. 460–473

7 BERGER, T.: 'Rate Distortion Theory' (Prentice-Hall, Englewood Cliffs, 1971)

8 BLAHUT, R. E.: 'Principles and Practice of Information Theory' (Addison-Wesley, MA, 1987)

30 Hz-LINEWIDTH, DIODE-LASER-PUMPED, Nd:GGG NONPLANAR RING OSCILLATORS BY ACTIVE FREQUENCY STABILISATION

Indexing terms: Lasers and laser applications, Oscillators, Optoelectronics

We report a heterodyne linewidth of less than 30 Hz for the beatnote between the outputs of two 282 THz (1·062 μm) Nd:GGG nonplanar ring oscillators (NPROs). The lasers were independently locked to adjacent axial modes of a high-finesse interferometer. The remnant frequency noise appears to be dominated by free spectral range fluctuations in the reference interferometer rather than by residual laser noise.

Stable lasers are necessary as local oscillators in many applications including coherent communications, high-resolution spectroscopy and gravity wave detection. Several helium neon, dye, and argon-ion lasers have been successfully stabilised for potential use in many of these fields.[1,2] In these lasers, however, the large free-running linewidths require wideband, complex, locking servos. In this letter we report on the active frequency stabilisation of monolithic, diode-laser-pumped, neodymium-doped gadolinium gallium garnet (Nd:GGG) ring lasers. These lasers have the advantage of a free-running noise bandwidth that is well below that of dye or argon-ion lasers. The servo requirements are therefore not as stringent.

Free-running linewidths of 3–10 kHz have been reported for Nd:YAG NPROs.[3,4] Diode laser pumping avoids the frequency noise associated with flashlamp pumping, and the unidirectional oscillation made possible by the nonplanar ring geometry avoids spatial hole-burning and improves resistance to optical feedback.[5] The lasers we stabilised were modified Lightwave Electronics model 120 NPROs with typical output powers of 2 mW.[6] The Nd:YAG crystals were replaced with Nd:GGG crystals optimised for improved resistance to optical feedback according to the eigenpolarisation theory developed by Nilsson *et al.*[5] PZT actuators were bonded directly to the Nd:GGG laser for rapid frequency control.[7] The PZT strain-induced laser tuning coefficient was 450 kHz/V, with a modulation bandwidth of 500 kHz and a maximum tuning range of 60 MHz. Additionally, the laser frequency could be tuned by adjusting the crystal temperature with a tuning rate of approximately -3 GHz/°C.

The apparatus is shown in Fig. 1 and uses a frequency discrimination technique known as Pound-Drever locking.[1,8,9] Laser 1 is phase modulated at a frequency f_1 of 40 MHz while laser 2 is phase modulated at a frequency f_2 of 61·5 MHz. The optical fields are mode-matched into a high-finesse interferometer (Newport Research Corp. model SR-150 SuperCavity). The reference cavity finesse is greater than 22 000, and the free spectral range is 6·327 GHz. The resulting transmission linewidth is therefore less than 300 kHz, so the frequency modulation sidebands lie outside the cavity transmission band and are reflected. A polarising beamsplitter and quarter-waveplate serve both to isolate the lasers from optical feedback and to

separate the incident and reflected waves. The resistance to optical feedback inherent in the NPRO design eliminates the need for further isolation.

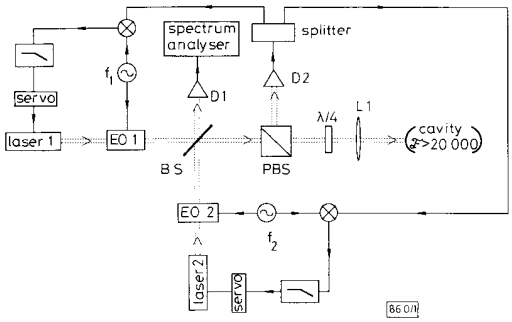

Fig. 1 *Experimental arrangement for simultaneously locking two lasers to one reference cavity and spectrally analysing resultant heterodyne beatnote*

The optical carrier frequency of laser 1 is locked in reflection to a resonance of the high-finesse interferometer. Using laser crystal temperature control the carrier frequency of laser 2 is tuned to an adjacent resonance of the interferometer. The carrier frequencies therefore differ by the free spectral range of the interferometer, 6·327 GHz. The reflected signal from each carrier has a strongly dispersive phase shift. These reflected carriers are optically mixed with their sidebands at the diode, creating IF signals at f_1 and f_2. The IF signals are then mixed with their respective RF drive sources in RF mixers to isolate electrically cross terms and to mix the dispersive error signals down to DC. Fig. 2 shows the error signals generated for each laser as the reference cavity resonance frequency is varied. The error signals are amplified by high-gain servos which feed back to the PZTs bonded to the laser crystals. The open loop gain of the system is 123 dB at DC with a unity gain frequency of 100 kHz. The controllers use cascaded integrators to provide high DC gain.

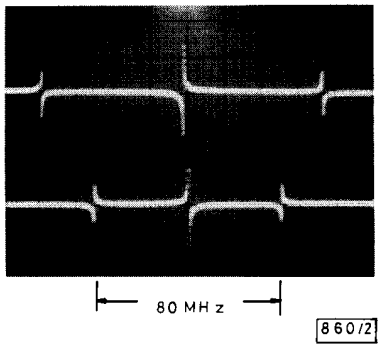

Fig. 2 *Error signals generated for each laser as reference cavity resonance frequency is varied about each laser's carrier frequency*

Lasers are frequency offset from each other by one reference cavity free spectral range (6·327 GHz)

Using this control system, both lasers were simulaneously locked to the interferometer for longer than one hour. This long-term locking was possible without an auxiliary low bandwidth loop for two reasons. First, the lasers were temperature-stabilised, and the reference cavity was temperature stabilised as well as hermetically sealed. This resulted in a long-term relative frequency drift of less than 1 MHz/min. Second, the error signal had the proper sign over a range of twice the phase modulation frequency which yielded a large dynamic range. Thus, the PZT actuator was adequate to provide long-term tracking.

The beatnote was detected with a wideband photodiode at the second port of beamsplitter BS and analysed on a Hewlett Packard model 8566B 22 GHz spectrum analyzer. Fig. 3 shows the resolution-limited 30 Hz linewidth obtained. The data shown are the video average of 10 sweeps for an integration time of 67 s. Even with this long integration time, the heterodyne linewidth is less than 30 Hz. The analysis of this type of locking shows that the shot-noise-limited linewidth is proportional to the square of the reference cavity linewidth and inversely proportional to the optical power.[9] When this analysis is applied to our system we find that the fundamental linewidth is approximately 500 μHz. Without video-averaging the data shown in Fig. 3 a large number of narrow spikes occur within the 30 Hz width. The presence of these spikes indicates that the observed experimental linewidth is probably due to small length changes in the reference cavity resulting in shifts of its free spectral range. We were unable to isolate electrically the reference cavity PZT, and 60 Hz pickup with an RMS value of the order of 1 mV, corresponding to length changes of 0·1 nm, is sufficient to account for the observed structure. This effect scales inversely with the square of the reference cavity length and would be reduced by using a longer interferometer.

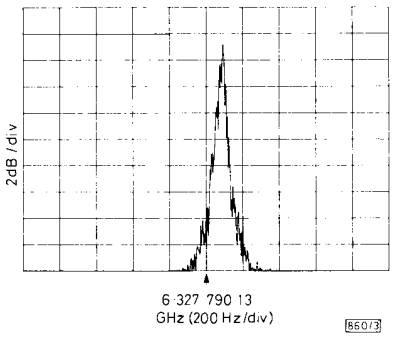

Fig. 3 *Heterodyne beatnote obtained under locked conditions*

Lasers are frequency offset by one reference cavity free spectral range (6·327 GHz). Data are video-averaged over 10 sweeps and resolution-limited to less than 30 Hz

The servo locking of our laser systems is robust. Highly reproducible beatnotes with linewidths less than 30 Hz were obtained, and locking times of greater than one hour were observed. We believe the observed linewidth is limited by fluctuations in the length of the reference cavity, and we are currently modifying the apparatus to reduce this effect. In future work we plan to measure the Allan variance of the heterodyne signal, and to provide a long-term frequency reference by locking the second harmonic of one of the lasers to a hyperfine transition in molecular iodine. Future efforts will also concentrate on investigating approaches for obtaining linewidths significantly below 30 Hz and reaching shot-noise-limited performance.

This work was supported by NASA under the SUNLITE program. A. D. Farinas thanks the National Science Foundation and C. D. Nabors thanks the Fannie and John Hertz Foundation for their support. We wish to thank Dr. J. Hall and his collaborators at the National Institute for Standards and Technology for many helpful discussions and Lightwave Electronics for the use of their lasers.

T. DAY
A. C. NILSSON
M. M. FEJER
A. D. FARINAS
E. K. GUSTAFSON
C. D. NABORS
R. L. BYER

Edward L. Ginzton Laboratory
Stanford University
Stanford, CA 94305, USA

12th April 1989

References

1 DREVER, R. W. P., HALL, J. L., KOWALSKI, F. V., HOUGH, J., FORD, G. M., MUNLEY, A. J., and WARD, H.: 'Laser phase and frequency stabilization using an optical resonator', *Appl. Phys. B*, 1983, **31**, pp. 97–105

2 MAN, C. N., and BRILLET, A.: 'Injection locking of argon-ion lasers', *Opt. Lett.*, 1984, **9**, pp. 333–334
3 KANE, T. J., NILSSON, A. C., and BYER, R. L.: 'Frequency stability and offset locking of a laser-diode pumped Nd:YAG monolithic nonplanar ring oscillator', *Opt. Lett.*, 1987, **12**, pp. 175–177
4 BUSH, S. P., GUNGOR, A., and DAVIS, C. C.: 'Studies of coherence properties of a diode-pumped Nd:YAG ring laser', *Appl. Phys. Lett.*, 1988, **53**, pp. 646–647
5 NILSSON, A. C., GUSTAFSON, E. K., and BYER, R. L.: 'Eigenpolarization theory of monolithic nonplanar ring oscillators', *J. Quantum Electron.*, 1989, **25**, pp. 767–790
6 Lightwave Electronics, 1161 San Antonio Rd., Mt. View, CA 94043
7 KANE, T. J., and CHENG, E. A. P.: 'Fast frequency tuning and phase locking of diode-pumped Nd:YAG ring lasers', *Opt. Lett.*, 1988, **13**, pp. 970–972
8 HOUGH, J., HILS, D., RAYMAN, M. D., MA, L. S., HOLLBERG, L., and HALL, J. L.: 'Dye-laser frequency stabilization using optical resonators', *Appl. Phys. B*, 1984, **33**, pp. 179–185
9 SALOMON, C., HILS, D., and HALL, J. L.: 'Laser stabilization at the millihertz level', *J. Opt. Soc. Am.*, 1988, **5**, pp. 1576–1587

IMPROVED RADIATION HARDNESS OF MOS DEVICES WITH ULTRATHIN NITRIDED OXIDE GATE DIELECTRICS PREPARED BY RAPID THERMAL PROCESSING

Indexing terms: Semiconductor devices and materials, MOS structures and devices, Dielectrics and dielectric devices, Radiation and radiation effects

The radiation hardness of MOS devices with ultrathin nitrided oxides (~100 Å) prepared by rapid thermal nitridation (RTN) of thin oxides has been studied. The radiation was performed by exposing devices under X-rays of 50 keV to a dose of 0·5 Mrad(Si). Compared with conventional thermal oxides, the RTN oxide devices exhibit a much smaller increase in both the fixed charge N_f and the interface state D_{it} densities. In addition, it is found that higher RTN temperature and/or longer durations produce smaller ΔN_f and ΔD_{it}.

Reliable thin gate dielectrics of nanometre-range thickness are critical to the development of future ULSI MOS technology. Oxynitride gate dielectrics prepared by various thermal nitridations of thermal oxides have received considerable attention as alternatives to thermally grown SiO_2. Superior characteristics over pure SiO_2 for gate dielectrics application have been reported. These include better resistance to impurity contaminations, effective barrier to dopant diffusion, reduced interface state generation under various electrical stresses, and insensitivity to radiation.[1–3] One of the most promising techniques for the formation of ultrathin oxynitride gate dielectrics is the rapid thermal nitridation (RTN) of thermal oxides due to its unique low thermal budget properties. Many papers have reported on the oxynitride device characteristics under various electrical stressing, but only few have reported on their radiation response. This letter reports the radiation effects in thin (~100 Å) oxides nitrided by RTN in terms of charge trapping and interface state generation. It is shown that the RTN devices exhibit a significantly improved radiation hardness over the control (thermal oxide) samples.

Oxides of ~100 Å thickness were thermally grown on *p*-type (100) Si wafers at 875°C. RTN was performed in pure NH_3 at 1 atm in a tungsten halogen lamp heating system. Polycrystalline silicon gate MOS capacitors with an area of 1×10^{-4} cm^2 were fabricated using standard processing. After aluminium deposition and patterning, samples were annealed at 450°C for 30 min in forming gas. All capacitors were then irradiated in a 50 keV X-ray system with 10 krad/min dose rate to a total dose of 0·5 Mrad(Si). Both high-frequency and quasistatic C/V measurements[4] were performed on devices before and immediately after irradiation.

A comparison between the control oxide as well as the RTN oxide (1100°C, 60 s) before and after irradiation at a total dosage of 0·5 Mrad(Si) is shown in Fig. 1. As can be seen, the RTN devices exhibit significantly less radiation-induced damage in terms of the shift of high-frequency C/V curves and the distortion of the quasistatic C/V curves. The C/V curves hardly change for RTN devices after irradiation, whereas a severe distortion of C/V curves is observed for the control oxide.

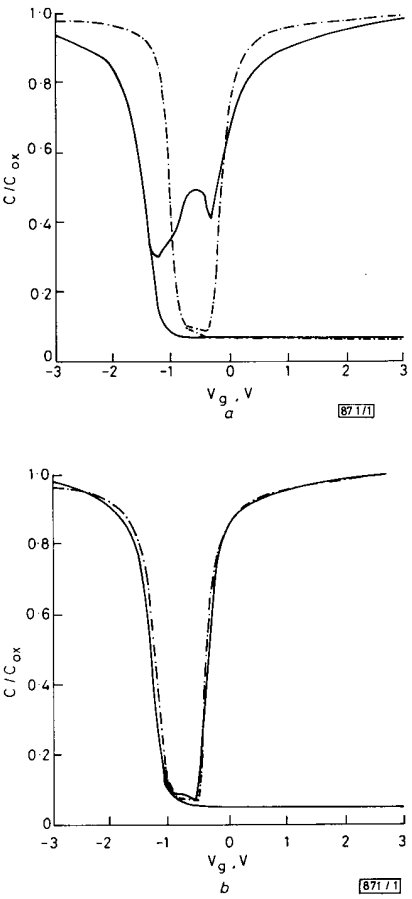

Fig. 1 *High-frequency and quasistatic C/V curves before and after X-ray irradiation at dose 0·5 Mrad(Si)*
a Control oxide
b RTN (1100°C, 60 s) oxide
—·—· before X-rays ——— after X-rays

We have examined the effect of RTN process parameters (time/temperature) on the change of midgap interface state density due to irradiation. As shown in Fig. 2, the interface state generation decreases as both the RTN temperature and time increase, except the 900°C, 10 s sample which shows a slight increase after irradiation. The increase of midgap interface state density in heavily nitrided oxides devices (1100°C, 60 s, 1200°C, 10–30 s) is nearly an order of magnitude smaller than that of the control oxide. For samples with RTN temperatures greater than 1000°C, a dramatic improvement has been observed even for nitridation times as short as 10 s.

Fig. 3 shows the flatband voltage shift (ΔV_{fb}) of MOS capacitors after 0·5 Mrad(Si) irradiation as a function of RTN process parameters. The flatband voltages were extracted from the high-frequency C/V measurements. The negative shift in V_{fb} is most likely due to the build-up of radiation-induced positive charges in the bulk as well as near the interface. A significant increase in D_{it} could also contribute to such a shift. However, for samples studied in this paper, the high-frequency C/V curves show parallel shifts rather than stretch-out distortions, except for the control oxide and the lightly nitrided